

Fermi surface studies of the skutterudite superconductors $\text{LaPt}_4\text{Ge}_{12}$ and $\text{PrPt}_4\text{Ge}_{12}$

B. Bergk,^{1,*} J. Klotz,^{1,2} T. Förster,¹ R. Gumeniuk,³ A. Leithe-Jasper,³ V. Lorenz,³ W. Schnelle,³ M. Nicklas,³ H. Rosner,³ Y. Grin,³ and J. Wosnitza^{1,2}

¹*Hochfeld-Magnetlabor Dresden (HLD-EMFL) and Würzburg-Dresden Cluster of Excellence ct.qmat, Helmholtz-Zentrum*

Dresden-Rossendorf, 01328 Dresden, Germany

²*Institut für Festkörper- und Materialphysik, TU Dresden, 01062 Dresden, Germany*

³*Max Planck Institute for Chemical Physics of Solids, 01187 Dresden, Germany*



(Received 28 March 2019; published 10 June 2019)

We report on comprehensive de Haas–van Alphen (dHvA) and electronic band-structure studies of the superconducting skutterudites $\text{LaPt}_4\text{Ge}_{12}$ ($T_c = 8.3$ K) and $\text{PrPt}_4\text{Ge}_{12}$ ($T_c = 7.9$ K). Both materials show very rich spectra of dHvA oscillations with similar and only slightly varying angular-dependent frequencies. The spectral richness can partly be rationalized by the elaborated electronic band structures resulting in several Fermi surfaces built by six different bands. The effective cyclotron masses of both superconductors lie between about 0.5 and 1.1 times the free-electron mass. Although these values are small, we find moderate mass enhancements between about 2 and 4 when comparing to the calculated masses. Our results evidence the localized character of the $4f$ electrons in the Pr compound and are in line with an electron-phonon mediated multiband superconductivity, largely identical for both compounds.

DOI: [10.1103/PhysRevB.99.245115](https://doi.org/10.1103/PhysRevB.99.245115)

I. INTRODUCTION

Compounds with rigid covalently bonded cage-forming frameworks have attracted much attention based on their diversity of fascinating physical phenomena observed. In particular, the family of filled skutterudites with the general formula MT_4X_{12} , where M is a rare-earth, alkali, or alkaline-earth metal, T a transition metal, and X a pnictogen (P, As, or Sb) or Ge, demonstrate remarkable properties (see [1–4] and references therein). One example worth mentioning is the first Pr-based heavy-fermion superconductor $\text{PrOs}_4\text{Sb}_{12}$ ($T_c = 1.85$ K) [5], with possibly having an unconventional order parameter with quadrupolar pairing [6].

Here, we focus on members of the filled skutterudite family MPt_4Ge_{12} with Pt-Ge framework. Superconductivity is found for quite a number of these skutterudites, namely for $M = \text{Sr}$, Ba, Th, La, and Pr [7–10]. The latter two materials have the highest transition temperatures in this family with $T_c = 8.3$ K for $\text{LaPt}_4\text{Ge}_{12}$ and $T_c = 7.9$ K for $\text{PrPt}_4\text{Ge}_{12}$ [10]. Contrary to the mentioned $\text{PrOs}_4\text{Sb}_{12}$, $\text{PrPt}_4\text{Ge}_{12}$ is not a heavy-fermion compound. Nevertheless, there are some indications for unconventional superconductivity, such as point-like nodes evidenced from NMR [11], specific-heat, and μSR penetration-depth measurements [12,13], as well as reports suggesting multiband superconductivity [13–18]. μSR measurements further evidenced the breaking of time-reversal symmetry in the superconducting state in $\text{PrPt}_4\text{Ge}_{12}$ [19,20], for which a complex singlet order parameter was discussed.

Time-reversal symmetry breaking is absent for $\text{LaPt}_4\text{Ge}_{12}$ [19]. For this material, most studies suggest the existence of

conventional superconductivity with a fully gapped pairing state [3,15,21,22] with somewhat weaker coupling than in $\text{PrPt}_4\text{Ge}_{12}$ [10]. Recent specific-heat and penetration-depth investigations showed indications of two-band superconductivity [22,23] which could not be ruled out as well in another thermodynamic study [3].

In an effort to shed more light on the electronic structure and on possible differences in the Fermi surface topologies and effective masses, we studied in great detail the magnetic quantum oscillations of the above compounds. In particular, we measured the de Haas–van Alphen (dHvA) effect and performed state-of-the-art band-structure calculations for $\text{LaPt}_4\text{Ge}_{12}$ and $\text{PrPt}_4\text{Ge}_{12}$. Our investigation evidences very similar band structures, Fermi surfaces, and effective masses for both compounds. The observed dHvA frequency spectra at high frequency are richer than calculated which indicates possible magnetic-breakdown orbits between the various bands crossing the Fermi surface or magnetic-interaction effects due to the large amplitudes of the observed quantum oscillations.

II. METHODS

High-quality crystals of $\text{LaPt}_4\text{Ge}_{12}$ and $\text{PrPt}_4\text{Ge}_{12}$ were grown starting from polycrystalline specimens, prepared by arc melting under Ar atmosphere, applying multistep thermal treatments. More details can be found in Refs. [3] and [14], respectively. The investigated samples had irregular shapes with mm-size dimensions. Mounting of the x-ray-oriented crystals was done carefully, but slight misalignments of a few degrees with respect to the magnetic field might easily have been possible.

The dHvA oscillations were measured by use of capacitive torque magnetometers employing CuBe cantilevers which were placed on rotatable platforms. The measurements were

*Present address: Institut für Werkstoffwissenschaft, TU Dresden, 01062 Dresden, Germany.

carried out at temperatures of about 40 mK in a dilution cryostat equipped with a superconducting 20 T magnet. For the determination of the effective masses in $\text{PrPt}_4\text{Ge}_{12}$ a ^3He cryostat with 15 T magnet was used.

Band-structure calculations were performed using the FPLO code (version 15.02-50) [24,25] with a scalar-relativistic setting. To approximate the exchange and correlation potential, we used the local density approximation of Perdew and Wang [26]. Both skutterudites crystallize in the cubic $Im\bar{3}$ (no. 204) structure. While the sites for La or Pr (0, 0, 0) and Pt (1/4, 1/4, 1/4) are fixed due to symmetry requirements, two of the coordinates of Ge (0, y_{Ge} , z_{Ge}) need to be determined. For $\text{LaPt}_4\text{Ge}_{12}$, the low-temperature experimental structural parameters $a = 8.611$ Å, $y_{\text{Ge}} = 0.1541$, and $z_{\text{Ge}} = 0.3554$ were used. For $\text{PrPt}_4\text{Ge}_{12}$, we used the room-temperature values $a = 8.6111$ Å, $y_{\text{Ge}} = 0.15127$, and $z_{\text{Ge}} = 0.35432$ reported in Ref. [27]. Note that our calculations are based on the stoichiometric composition of both compounds, which is within error bars of the values $\text{La}_{0.9(1)}\text{Pt}_{3.9(1)}\text{Ge}_{12.1(1)}$ and $\text{Pr}_{1.1(1)}\text{Pt}_{4.0(1)}\text{Ge}_{11.9(1)}$ reported in Ref. [27]. The $4f$ electrons of Pr were treated as core electrons. We used a $28 \times 28 \times 28$ k mesh for calculating the self-consistent density and a seven (four) times denser grid for extracting the extremal Fermi surface cross sections of the La (Pr) compound.

III. RESULTS AND DISCUSSION

Typical magnetic-field-dependent torque signals measured at ~ 40 mK are shown in Fig. 1(a) for $\text{LaPt}_4\text{Ge}_{12}$ and in Fig. 1(b) for $\text{PrPt}_4\text{Ge}_{12}$. At low fields, in the superconducting state, large torque signals are detected, with sharp peaks appearing just before the normal state is reached at $\mu_0 H_{c2} = 1.40$ T for $\text{LaPt}_4\text{Ge}_{12}$ and $\mu_0 H_{c2} = 1.69$ T for $\text{PrPt}_4\text{Ge}_{12}$. The peaks in the magnetization indicate a massive rearrangement of vortices in the Shubnikov phase. This so-called peak effect has been well known for more than 50 years [28,29] and occurs in many type-II superconductors [30,31].

Towards higher magnetic fields, clear dHvA oscillations emerge for both materials. In the Fourier transformations (insets of Fig. 1), a large number of dHvA frequencies are resolved. The spectral richness and the closeness of some of the dHvA frequencies make the determination and assignment of “real” dHvA frequencies challenging. In the data shown in Fig. 1, a number of frequencies cluster below about 300 T and another bunch between 1100 and 2200 T. The similarity of the torque signals and of the spectral distribution of the dHvA frequencies for both materials is obvious.

When rotating the crystals with respect to the magnetic fields, the general form of the torque signals changes only marginally. For all angles measured, and for both compounds, the clustering of the dHvA frequencies remains, with up to six frequencies appearing below 630 T and up to about 10 frequencies lying between 1100 and ~ 2500 T (Fig. 2) [32]. Only the number of observed frequencies and the relative amplitudes of the dHvA oscillations show some angular and material dependence. The similar angular dependences of the dHvA spectra for $\text{LaPt}_4\text{Ge}_{12}$ and $\text{PrPt}_4\text{Ge}_{12}$ is again striking. This evidences very similar Fermi surface topologies for both materials.

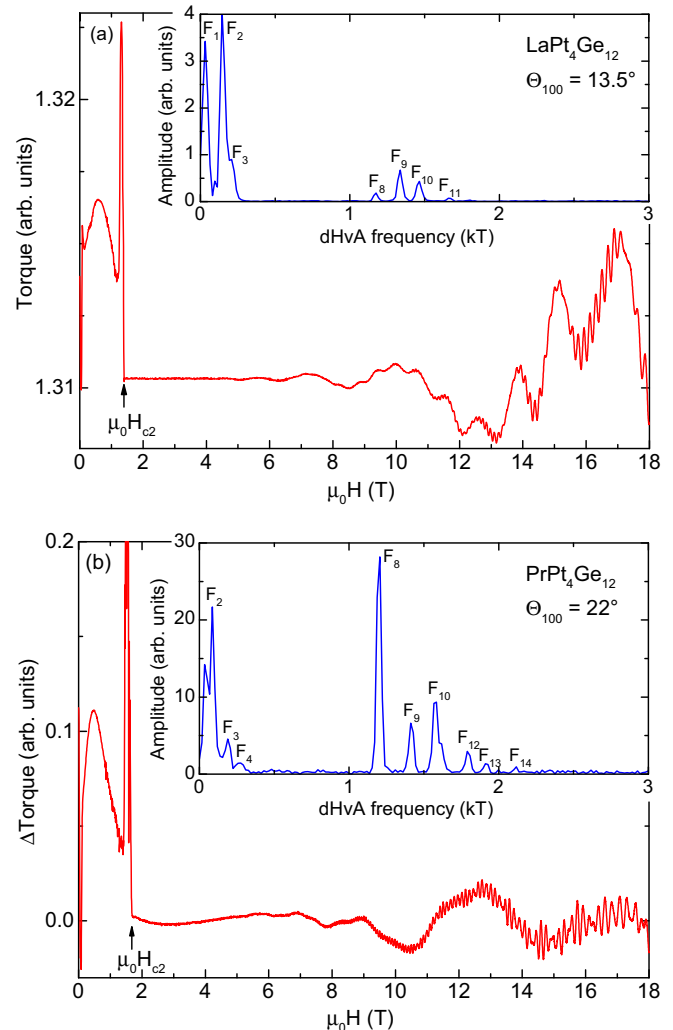


FIG. 1. Field-dependent torque magnetization of (a) $\text{LaPt}_4\text{Ge}_{12}$ and (b) $\text{PrPt}_4\text{Ge}_{12}$ measured at ~ 40 mK for magnetic fields aligned for the stated angles within the bc plane, with $\Theta_{100} = 0$ for field aligned along the [001] direction. For $\text{PrPt}_4\text{Ge}_{12}$ a smooth background (fourth-order polynomial) was subtracted. The insets show the Fourier transforms of the torque data between 8.5 and 18 T after background subtraction.

After having extracted the rich dHvA spectra we compare our experimental data to calculated extremal orbits, i.e., expected quantum-oscillation frequencies, by use of state-of-the-art band-structure calculations. Figure 3 shows the calculated dispersion relations for selected symmetry directions, as shown in the insets. The band structures of both materials are nearly identical. Six bands, highlighted by different colors, are crossing the Fermi energy, E_F , sometimes at multiple points along the symmetry directions. In Fig. 3, we as well show the calculated density of states (right panels). The Ge $4p$ states are the main contributors at E_F with some admixture of Pt $5d$ and other states. Our results are in line with earlier results [10], although we obtain somewhat smaller values for the density of states at E_F , $D(E_F)$, with 11 and 9 states/eV, compared to 13.4 and 9.3 states/eV in [10], for $\text{LaPt}_4\text{Ge}_{12}$ and $\text{PrPt}_4\text{Ge}_{12}$, respectively. In a recent density-functional-theory study on La-containing filled skutterudites $D(E_F) =$

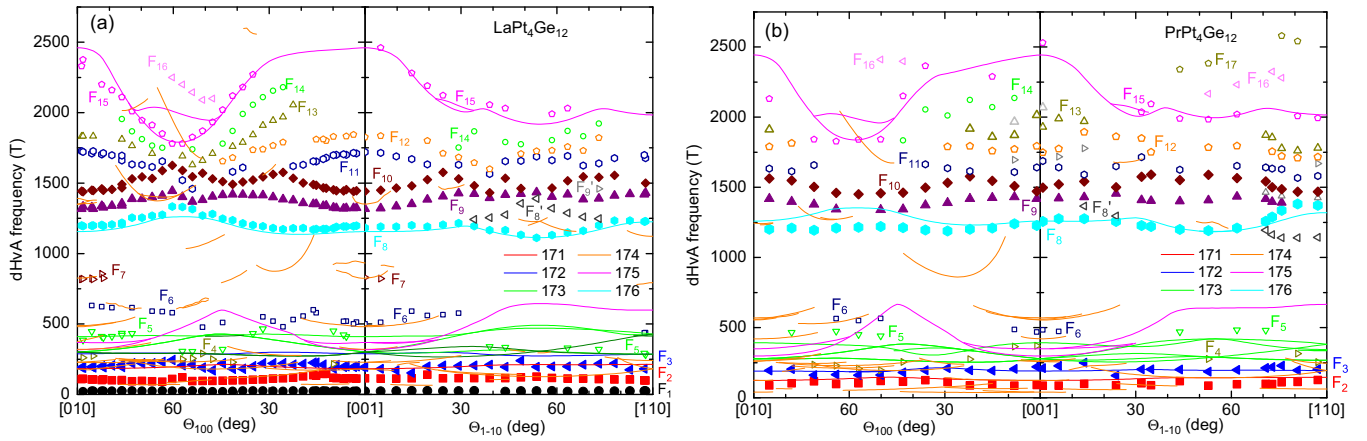


FIG. 2. Angular dependence of the dHvA frequencies of (a) LaPt₄Ge₁₂ and (b) PrPt₄Ge₁₂. The symbols are experimental data from Fourier transformations and the solid lines represent the calculated frequencies using the FPLO code. As shown in Fig. 3, the bands 171 to 176 are crossing the Fermi energy. We have chosen corresponding colors for the calculated dispersion relations and the calculated dHvA frequencies, originating from the respective bands.

9.60 states/eV was reported for LaPt₄Ge₁₂ [4]. From our calculated density of states and using the equation $\gamma_{calc} = \pi^2 k_B^2 D(E_F)/3$, with the Boltzmann constant k_B , we determine the Sommerfeld coefficients 25 mJ/(mol K²) for LaPt₄Ge₁₂ and 20 mJ/(mol K²) for PrPt₄Ge₁₂. Experimentally, γ values between 50 and 76 mJ/(mol K²) for the La compound [3,10,22] and between 45 and 107 mJ/(mol K²) for the Pr compound were reported [10,12,14,17,18,33]. Since in the calculated values no many-body interactions are included, the larger experimental values, although considerably scattered, suggest mass-enhancement factors, $\gamma/\gamma_{calc} = 1 + \lambda_\gamma$,

between 2 and 3.0 for the La and 2.2 to 5.3 for the Pr compound. We will come back to this when discussing the calculated and experimentally determined effective masses.

The strongly dispersive band structures with six bands crossing E_F lead to highly evolved Fermi surface topologies. The resulting Fermi surface sheets are shown inside the first Brillouin zone for each band separately in Fig. 4, using corresponding colors for the respective bands as shown in Fig. 3. As expected from the similar band structures, there is almost no difference visible in the Fermi surface sheets for both materials. The red, blue, and cyan ellipsoidal (or nearly spherical) Fermi surfaces originate from the bands 171, 172, and 176, respectively, and lead to single extremal orbits each. The bands 173 (green) and 175 (magenta) lead to multiple Fermi surfaces with a number of extremal orbits appearing over the whole angular range. Band 174 (orange) results in a multiple-connected Fermi surface “monster” with a large number of extremal orbits appearing only over restricted angular regions. Thereby, the charge carriers of the bands 171, 172, and 173 are holelike and electronlike for the bands 175 and 176. The monster comprises electron- and holelike orbits. The resulting calculated angular-dependent dHvA frequencies are plotted as solid lines, with corresponding colors, in Fig. 2.

For many of the dHvA signals, we find a reasonable agreement between theory and experiment. There are, however, as well some unexplained experimental frequencies. In line with the experiments, the calculations result in a number of extremal orbits (from bands 171, 172, 173, and 175) lying below about 650 T, a region up to ~ 1100 T with no or sparse orbits (only from the monster band 174), and between 1100 and 2500 T the orbits labeled F_8 from band 176 and F_{15} from band 175. From calculation, there are as well some extremal orbits from band 174 predicted to occur over restricted angular regions at higher frequencies up to about 4500 T, i.e., above the range shown in Fig. 2. No dHvA oscillations could be resolved at these high frequencies in our experiments.

If we compare calculations and experiments in more detail, we find in the low-frequency region (below ~ 650 T) more

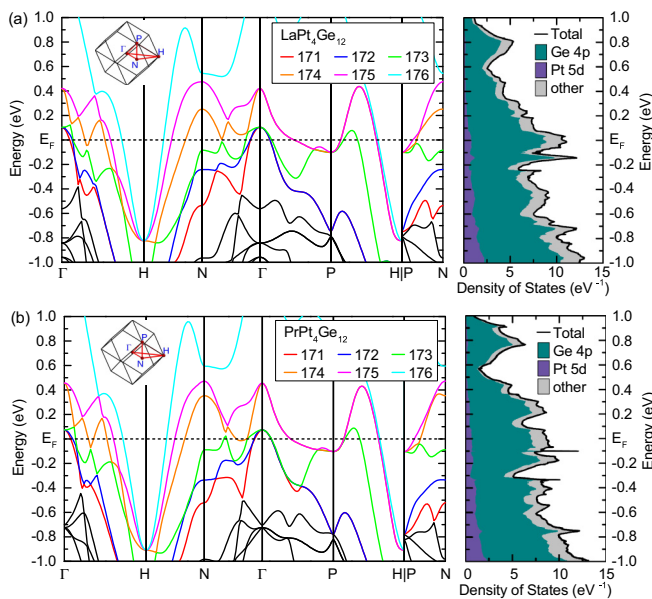


FIG. 3. (Left panels) Calculated band structure for (a) LaPt₄Ge₁₂ and (b) PrPt₄Ge₁₂. The dashed lines indicate the Fermi energy, E_F . The insets show the first Brillouin zone with high-symmetry points. The right panels show the calculated total and atom-orbital selected density of states. The dominant contribution at E_F originates from the Ge 4p orbitals.

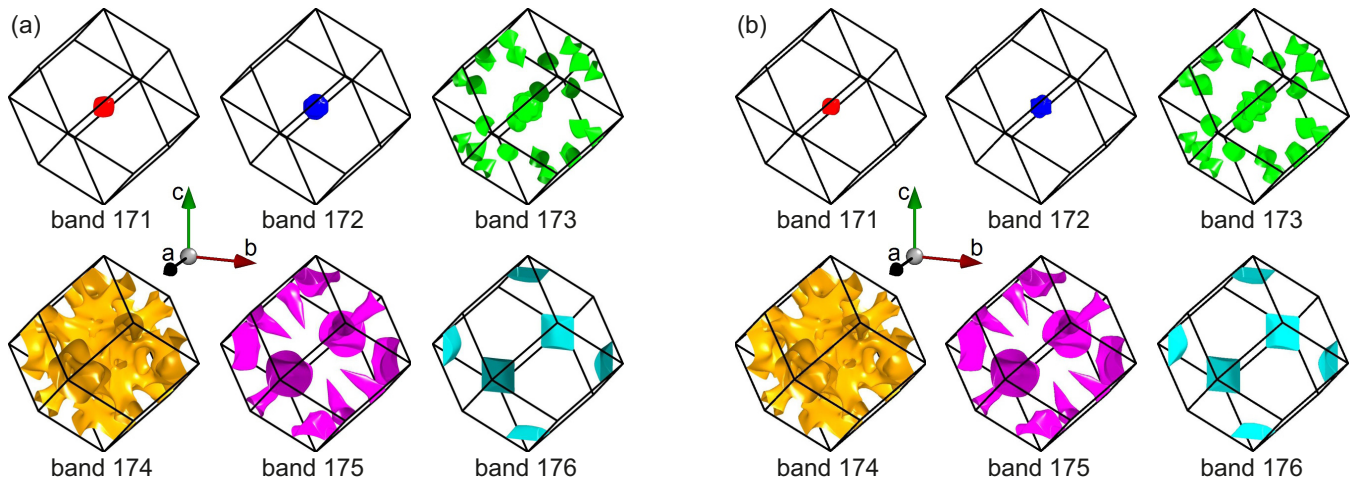


FIG. 4. Calculated Fermi surfaces for (a) $\text{LaPt}_4\text{Ge}_{12}$ and (b) $\text{PrPt}_4\text{Ge}_{12}$ inside the first Brillouin zone (black lines). For each band, corresponding colors have been chosen for the Fermi surfaces, for the calculated extremal orbits (Fig. 2), and for the dispersion relations (Fig. 3).

dHvA frequencies predicted than observed. We assign the orbits F_2 and F_3 to the small spherical Fermi surfaces of the bands 171 and 172, respectively. The experimental values are somewhat smaller than the calculated ones which is not unusual for such tiny Fermi surfaces and might be easily explained by small changes in the band dispersions or band fillings. Indeed, the discrepancies are small when comparing the absolute numbers; see also Table I. For $\text{LaPt}_4\text{Ge}_{12}$, a very small orbit F_1 of about 25 T was observed that has no obvious counterpart in the calculation, possibly due to the same reason. In the intermediate frequency region, F_6 and F_7 fit to calculated orbits from band 174. In experiment, the amplitudes of these dHvA frequencies are rather weak indicating large effective masses, high scattering rates, or unfavorable curvature factors. It is reasonable to assume that a combination of these factors makes the orbits on the multiconnected monster Fermi surface hard to resolve, especially when lying close to other large-amplitude dHvA signals from other bands. Furthermore, small deviations from the stoichiometry may lead to slight alterations of the Fermi energy, which may also explain some discrepancies between calculation and experiment.

In the high-frequency range, between 1100 and 2500 T, we surprisingly find much more dHvA frequencies in experiment than in theory (Fig. 2). Such observation is more difficult to rationalize than to explain missing dHvA signals in experiment, as just done for the expected orbits from band 174. One possibility for the occurrence of additional quantum oscillations in experiment is magnetic breakdown [34]. Thereby electrons tunnel from one band to another band close by in large applied magnetic field. In the present compounds, the large number of bands crossing the Fermi energy leads to many tunneling possibilities in k space. The complicated Fermi surface topology makes an assignment of possible breakdown orbits, however, hardly possible. Another cause for additional dHvA frequencies is magnetic interaction [34]. This effect occurs when magnetization oscillations with large amplitude, \tilde{M} , lead to multiple values of the internal magnetic flux density, $B = \mu_0[H + \tilde{M}(B)]$, with $\mu_0 H$ the applied magnetic field. This, consequently, results in additional frequencies that are sums

or differences of real dHvA frequencies, as has been observed, for instance, in such a simple metal as indium [35]. Here,

TABLE I. dHvA frequencies and effective masses for various extremal orbits in $\text{LaPt}_4\text{Ge}_{12}$ and $\text{PrPt}_4\text{Ge}_{12}$ for the given magnetic-field directions from experiment and, where possible, from calculation.

Orbit	F (T)		$ m^* $ (m_e)		λ	Band
	Expt.	Calc.	Expt.	Calc.		
$\text{LaPt}_4\text{Ge}_{12}$, $\Theta_{100} = 18^\circ$						
F_1	25		0.48(6)			
		72		0.29		174
		160		0.22		174
		173		0.67		174
F_2	133	189	0.47(11)	0.22	1.1	171
		273		0.34		173
F_3	225	297	1.1(2)	0.24	3.6	172
F_6	580	528	1.13(7)	0.62	0.8	174
		1034		0.89		174
F_8	1174	1137	0.6(1)	0.24	1.5	176
F_9	1352		0.53(4)			
F_{10}	1585		0.64(5)			
F_{11}	1653		0.61(2)			
F_{15}		2433		0.59		175
$\text{PrPt}_4\text{Ge}_{12}$, $\Theta_{100} = 66^\circ$						
F_2	105	132	0.57(9)	0.22	1.6	171
F_3	164	187		0.32		172
		220		0.40		174
F_4	229	230		0.34		174
		247		0.38		174
		402		0.52		175
		534		0.40		174
		1269		0.78		174
F_8	1165	1342	0.48(3)	0.28	0.7	176
F_{10}	1456		0.90(7)			
F_{15}	1804	1896	0.8(2)	0.41	1.0	175

we indeed observe large-amplitude dHvA signals (Fig. 1) that may give rise to magnetic interaction. In any case, for either magnetic breakdown or magnetic interaction, the additional oscillation frequencies are not given by extremal orbits on the calculated Fermi surfaces.

In a further step, we determined the effective masses of the observed cyclotron orbits at selected angles. For that, we measured the temperature dependences of the dHvA oscillation amplitudes, extracted from Fourier transformations, and used the usual Lifshitz-Kosevich temperature damping factor [34,36] $R_T = x/\sinh x$, with $x = \alpha T m^*/B$, $\alpha = 2\pi^2 k_B m_e / (e\hbar) = 14.69$ T/K, and m^* the effective mass in units of the free-electron mass, m_e , to describe the data. Here, e is the electron charge and \hbar the reduced Planck constant. The resultant masses are compared with calculated band masses, m_b , and shown, together with experimental and calculated dHvA frequencies, in Table I. The measured effective masses lie between 0.47 and 1.13 free electron masses which gives mass-enhancement factors $m^*/m_b = 1 + \lambda$ between about 2 and 4. This is in line with the enhancement factors deduced from the specific heat (see above). We find somewhat smaller enhancements in λ compared to λ_γ for PrPt₄Ge₁₂, but that may be well within error bars. It is reasonable to assume that the major part of the mass enhancements is due to electron-phonon coupling that as well is causing Cooper pairing [4]. The relatively high T_c of the two compounds fit with the found large λ values. The suggested multiband superconductivity [3,13–18,22,23] is as well supported by our finding of multiple (six) bands crossing the Fermi energy showing different mass enhancements.

IV. CONCLUSION

Our de Haas–van Alphen measurements in combination with state-of-the-art band-structure calculations evidence that the electronic structures of LaPt₄Ge₁₂ and PrPt₄Ge₁₂ are nearly identical. Both materials show rich dHvA spectra with moderately enhanced effective masses. Most of the observed quantum oscillations can be explained by our calculations. Some of the observed oscillations, however, are assumed to be caused either by magnetic breakdown or magnetic interaction. The observed mass enhancements are in line with electron-phonon mediated Cooper pairing of different strengths for the six bands crossing the Fermi energy. We point out that, consequently, a correct description of the superconducting gap structure of these two compounds requires a complex multi-band model possessing a large number of parameters which are not independently experimentally accessible. This renders the interpretation of experimental data regarding properties such as the superconducting gap structure challenging. Thus some of the existing evidence concerning the gap structures and other superconducting properties might need to be reconsidered [12–16].

ACKNOWLEDGMENTS

We acknowledge support by HLD at HZDR, member of the European Magnetic Field Laboratory (EMFL), from the ANR-DFG grant “Fermi-NEST”, and from the DFG through the Würzburg-Dresden Cluster of Excellence on Complexity and Topology in Quantum Matter–*ct.qmat* (EXC 2147, Project No. 39085490).

-
- [1] M. B. Maple, E. D. Bauer, N. A. Frederick, P.-C. Ho, W. A. Yuhasz, and V. S. Zapf, *Physica B* **328**, 29 (2003).
 - [2] Y. Aoki, H. Sugawara, H. Hisatomo, and H. Sato, *J. Phys. Soc. Jpn.* **74**, 209 (2005).
 - [3] H. Pfau, M. Nicklas, U. Stockert, R. Gumeniuk, W. Schnelle, A. Leithe-Jasper, Y. Grin, and F. Steglich, *Phys. Rev. B* **94**, 054523 (2016).
 - [4] H. M. Tütüncü, E. Karaca, and G. P. Srivastava, *Phys. Rev. B* **95**, 214514 (2017).
 - [5] E. D. Bauer, N. A. Frederick, P.-C. Ho, V. S. Zapf, and M. B. Maple, *Phys. Rev. B* **65**, 100506(R) (2002).
 - [6] R. Vollmer, A. Faïß t, C. Pfeleiderer, H. v. Löhneysen, E. D. Bauer, P.-C. Ho, V. Zapf, and M. B. Maple, *Phys. Rev. Lett.* **90**, 057001 (2003).
 - [7] E. Bauer, A. Grytsiv, X.-Q. Chen, N. Melnychenko-Koblyuk, G. Hilscher, H. Kaldarar, H. Michor, E. Royanian, G. Giester, M. Rotter, R. Podloucky, and P. Rogl, *Phys. Rev. Lett.* **99**, 217001 (2007).
 - [8] E. Bauer, X.-Q. Chen, P. Rogl, G. Hilscher, H. Michor, E. Royanian, R. Podloucky, G. Giester, O. Sologub, and A. P. Gonçalves, *Phys. Rev. B* **78**, 064516 (2008).
 - [9] D. Kaczorowski and V. H. Tran, *Phys. Rev. B* **77**, 180504(R) (2008).
 - [10] R. Gumeniuk, W. Schnelle, H. Rosner, M. Nicklas, A. Leithe-Jasper, and Y. Grin, *Phys. Rev. Lett.* **100**, 017002 (2008).
 - [11] F. Kanetake, H. Mukuda, Y. Kitaoka, K. Magishi, H. Sugawara, K. M. Itoh, and E. E. Haller, *J. Phys. Soc. Jpn.* **79**, 063702 (2010).
 - [12] A. Maisuradze, M. Nicklas, R. Gumeniuk, C. Baines, W. Schnelle, H. Rosner, A. Leithe-Jasper, Y. Grin, and R. Khasanov, *Phys. Rev. Lett.* **103**, 147002 (2009).
 - [13] Y. P. Singh, R. B. Adhikari, S. Zhang, K. Huang, D. Yazici, I. Jeon, M. B. Maple, M. Dzero, and C. C. Almasan, *Phys. Rev. B* **94**, 144502 (2016).
 - [14] J. L. Zhang, Y. Chen, L. Jiao, R. Gumeniuk, M. Nicklas, Y. H. Chen, L. Yang, B. H. Fu, W. Schnelle, H. Rosner, A. Leithe-Jasper, Y. Grin, F. Steglich, and H. Q. Yuan, *Phys. Rev. B* **87**, 064502 (2013).
 - [15] Y. Nakamura, H. Okazaki, R. Yoshida, T. Wakita, H. Takeya, K. Hirata, M. Hirai, Y. Muraoka, and T. Yokoya, *Phys. Rev. B* **86**, 014521 (2012).
 - [16] L. S. Sharath Chandra, M. K. Chattopadhyay, and S. B. Roy, *Supercond. Sci. Technol.* **25**, 105009 (2012).
 - [17] K. Huang, L. Shu, I. K. Lum, B. D. White, M. Janoschek, D. Yazici, J. J. Hamlin, D. A. Zocco, P.-C. Ho, R. E. Baumbach, and M. B. Maple, *Phys. Rev. B* **89**, 035145 (2014).
 - [18] I. Jeon, S. Ran, A. J. Breindel, P.-C. Ho, R. B. Adhikari, C. C. Almasan, B. Luong, and M. B. Maple, *Phys. Rev. B* **95**, 134517 (2017).

- [19] A. Maisuradze, W. Schnelle, R. Khasanov, R. Gumeniuk, M. Nicklas, H. Rosner, A. Leithe-Jasper, Y. Grin, A. Amato, and P. Thalmeier, *Phys. Rev. B* **82**, 024524 (2010).
- [20] J. Zhang, D. E. MacLaughlin, A. D. Hillier, Z. F. Ding, K. Huang, M. B. Maple, and L. Shu, *Phys. Rev. B* **91**, 104523 (2015).
- [21] M. Toda, H. Sugawara, K. Magishi, T. Saito, K. Koyama, Y. Aoki, and H. Sato, *J. Phys. Soc. Jpn.* **77**, 124702 (2008).
- [22] K. Huang, D. Yazici, B. D. White, I. Jeon, A. J. Breindel, N. Pouse, and M. B. Maple, *Phys. Rev. B* **94**, 094501 (2016).
- [23] J. L. Zhang, G. M. Pang, L. Jiao, M. Nicklas, Y. Chen, Z. F. Weng, M. Smidman, W. Schnelle, A. Leithe-Jasper, A. Maisuradze, C. Baines, R. Khasanov, A. Amato, F. Steglich, R. Gumeniuk, and H. Q. Yuan, *Phys. Rev. B* **92**, 220503(R) (2015).
- [24] K. Koepf and H. Eschrig, *Phys. Rev. B* **59**, 1743 (1999).
- [25] <http://www.fplo.de/>
- [26] J. P. Perdew and Y. Wang, *Phys. Rev. B* **45**, 13244 (1992).
- [27] R. Gumeniuk, H. Borrmann, A. Ormeci, H. Rosner, W. Schnelle, M. Nicklas, Y. Grin, and A. Leithe-Jasper, *Z. Kristallogr.* **225**, 531 (2010).
- [28] W. DeSorbo, *Rev. Mod. Phys.* **36**, 90 (1964).
- [29] A. B. Pippard, *Philos. Mag.* **19**, 217 (1969).
- [30] M. Marchevsky, M. J. Higgins, and S. Bhattacharya, *Nature (London)* **409**, 591 (2001).
- [31] J. Nössler, R. Seerig, S. Yasin, M. Uhlarz, S. Zherlitsyn, G. Behr, S.-L. Drechsler, G. Fuchs, H. Rosner, and J. Wosnitza, *Phys. Rev. B* **95**, 014523 (2017).
- [32] For LaPt₄Ge₁₂, another weak dHvA signal, labeled F_7 , appears at about 825 T in a very narrow angular range.
- [33] I. Jeon, K. Huang, D. Yazici, N. Kanchanavatee, B. D. White, P.-C. Ho, S. Jang, N. Pouse, and M. B. Maple, *Phys. Rev. B* **93**, 104507 (2016).
- [34] D. Shoenberg, *Magnetic Oscillations in Metals* (Cambridge University Press, Cambridge, UK, 1984).
- [35] J. H. P. van Weeren and J. R. Anderson, *J. Phys. F: Met. Phys.* **3**, 2109 (1973).
- [36] I. M. Lifshitz and A. M. Kosevich, *Zh. Eksp. Teor. Fiz.* **29**, 730 (1956) [*Sov. Phys. JETP* **2**, 636 (1956)].